View metadata, citation and similar papers at core.ac.uk
brought to you by CORE
provided by Elsevier - Publisher Connector

Structure, Vol. 13, 1081–1088, July, 2005, ©2005 Elsevier Ltd All rights reserved. DOI 10.1016/j.str.2005.04.023

Structural Basis for Substrate Specificity of the Human Mitochondrial Deoxyribonucleotidase

Karin Walldén,[1,2,4] Benedetta Ruzzenente,[3,4] Agnes Rinaldo-Matthis,[1] Vera Bianchi,[3] and Pär Nordlund[1,2,*]

[1]Department of Biochemistry and Biophysics
Stockholm University
SE-106 91 Stockholm
Sweden

[2]Department of Medical Biochemistry and Biophysics
Karolinska Institutet
SE-171 77 Stockholm
Sweden

[3]Department of Biology
University of Padova
I-35131 Padova
Italy

Summary

The human mitochondrial deoxyribonucleotidase catalyzes the dephosphorylation of thymidine and deoxyuridine monophosphates and participates in the regulation of the dTTP pool in mitochondria. We present seven structures of the inactive D41N variant of this enzyme in complex with thymidine 3′-monophosphate, thymidine 5′-monophosphate, deoxyuridine 5′-monophosphate, uridine 5′-monophosphate, deoxyguanosine 5′-monophosphate, uridine 2′-monophosphate, and the 5′-monophosphate of the nucleoside analog 3′-deoxy 2′3′-didehydrothymidine, and we draw conclusions about the substrate specificity based on comparisons with enzyme activities. We show that the enzyme's specificity for the deoxyribo form of nucleoside 5′-monophosphates is due to Ile-133, Phe-49, and Phe-102, which surround the 2′ position of the sugar and cause an energetically unfavorable environment for the 2′-hydroxyl group of ribonucleoside 5′-monophosphates. The close binding of the 3′-hydroxyl group of nucleoside 5′-monophosphates to the enzyme indicates that nucleoside analog drugs that are substituted with a bulky group at this position will not be good substrates for this enzyme.

Introduction

The DNA replication machinery requires a balanced supply of the four deoxyribonucleoside triphosphates (dNTPs) to carry out a correct DNA synthesis. The cell uses the complex allosteric regulation of ribonucleotide reductase and the action of various enzymes such as nucleoside and nucleotide kinases and 5′-nucleotidases to control dNTP pool sizes (Jordan and Reichard, 1998). Here, we focus on the mitochondrial deoxyribonucleotidase (mdN, previously named dNT-2) (Rampazzo et al., 2000a; Bianchi and Spychala, 2003), one of seven known human 5′-nucleotidases that catalyze the dephosphorylation of nucleoside monophosphates to nucleosides and inorganic phosphate. The general properties of 5′-nucleotidases have recently been reviewed (Bianchi and Spychala, 2003). Although their substrate specificities are rather broad and partially overlapping, individual 5′-nucleotidases show differences in substrate specificity and subcellular location. However, with the exception of the ecto-5′-nucleotidase (eN), they all have a common sequence motif, DXDXV/T, in their active site and depend on Mg^{2+} for activity, which indicates a similar catalytic mechanism (Bianchi and Spychala, 2003).

The enzyme mdN is the only 5′-nucleotidase found so far in mitochondria and prefers thymidine 5′-monophosphate (dTMP5′), deoxyuridine 5′-monophosphate (dUMP5′), thymidine 3′-monophosphate (dTMP3′), and uridine 3′-monophosphate (UMP3′) as substrates (Rampazzo et al., 2000a; Gallinaro et al., 2002; Mazzon et al., 2003). The sequence of mdN is 52% identical to that of the cytosolic deoxyribonucleotidase (cdN, previously named dNT-1) (Rampazzo et al., 2000b; Bianchi and Spychala, 2003), which is active with the same substrates as those used by mdN but is also active with deoxyguanosine 5′-monophosphate (dGMP5′) and deoxyinosine 5′monophosphate (dIMP5′) (Höglund and Reichard, 1990; Rampazzo et al., 2000b). These two enzymes are the only known 5′-nucleotidases that prefer the 2′-deoxyribo form over the ribo form of nucleoside 5′-monophosphates. The activity of mdN on non-nucleoside phosphates has never been tested, but cdN has been shown to be active with p-nitrophenyl phosphate and inactive with β-glycerophosphate, glucose-6-phosphate, carbamoylphosphate, creatine phosphate, and tetrasodium pyrophosphate (Höglund and Reichard, 1990).

5′-nucleotidases influence the input of nucleotides into the cellular pools by reversing the reaction catalyzed by nucleoside kinases. The two deoxyribonucleotidases, cdN and mdN, have been shown to modulate the phosphorylation of thymidine and deoxyuridine by creating regulatory substrate cycles with the cytosolic (Bradshaw and Deininger, 1984) and mitochondrial (Johansson and Karlsson, 1997) thymidine kinases, respectively (Gazziola et al., 2001; Rampazzo et al., 2004). The physiological function of 5′-nucleotidases is however still incompletely clarified. A role in the catabolism of macromolecular nucleic acids is recognized for cN-III, a pyrimidine-specific 5′-nucleotidase specifically expressed in red blood cells (Marinaki et al., 2001; Bianchi and Spychala, 2003). A similar function may be performed by other 5′-nucleotidases in other cell types.

5′-nucleotidases participate in the metabolism of nucleoside analog drugs. Many antiviral and anticancer nucleoside analogs are activated by phosphorylation to their 5′-triphosphates and are then incorporated into the DNA of the tumor cell or virus, where they primarily act as DNA chain terminators. Nucleoside and nucleotide kinases and 5′-nucleotidases control the level of phosphorylation of the nucleoside analogs (Wang et al., 1999; Mazzon et al., 2003; Van Rompay et al., 2003) and

*Correspondence: par@dbb.su.se
[4]These authors contributed equally to this work.

therefore their pharmacological effect. Deoxyribonucleoside kinases and deoxyribonucleotidases show a wide range of activities with different nucleoside analogs (Wang et al., 1999; Mazzon et al., 2003; Van Rompay et al., 2003). To be effective, a nucleoside analog should be a good substrate for the kinases and be dephosphorylated poorly by the 5′-nucleotidases.

Several anti-HIV nucleoside analogs, e.g., 3′-azido 3′-thymidine (AZT) and 3′-deoxy 2′3′-didehydrothymidine (d4T), show mitochondrial toxicity (Lewis and Dalakas, 1995) generally attributed to incorporation of the analogs into mtDNA, which leads to DNA damage and mtDNA depletion (Tozser, 2001). In fact, the triphosphate form of anti-HIV nucleoside analogs such as AZT and d4T can be incorporated into mtDNA by DNA polymerase γ (Feng et al., 2001; Johnson et al., 2001; Lim and Copeland, 2001). Overexpression of the inner membrane nucleoside transporter ENT1 leads to an increased incorporation of antiviral nucleoside analogs into mtDNA (Lai et al., 2004). To reduce the mitochondrial toxicity of nucleoside analogs, the concentration of their phosphates in mitochondria should be kept low. This may possibly be accomplished by constructing nucleoside analogs that are easily dephosphorylated by mdN. The monophosphate form of AZT (AZTMP) and d4T (d4TMP) are in fact dephosphorylated poorly by mdN (Mazzon et al., 2003).

The structure of mdN (Rinaldo-Matthis et al., 2002) was the first structure determined of a mammalian 5′-nucleotidase, and it was determined with inorganic phosphate in the active site and also with the product thymidine trapped together with beryllium trifluoride (BeF_3^-) (Rinaldo-Matthis et al., 2002). Thymidine binds with the 3′-hydroxyl group toward the BeF_3^-, indicating that the corresponding substrate would be dTMP3′. The catalytic mechanism of mdN was outlined, and several relevant amino acids, water molecules, and cofactors for substrate recognition were identified (Rinaldo-Matthis et al., 2002).

The aim of the present study was to further investigate the structural basis for substrate specificity of mdN by (1) looking at the difference in binding of substrates phosphorylated at the 2′-, 3′-, and 5′-position of the ribose and (2) comparing the binding of various nucleoside 5′-monophosphates. To achieve our aims, we used site-directed mutagenesis to produce an inactive mdN variant, D41N, in which substrates are bound but not dephosphorylated. Here, we present seven structures of the D41N variant in complex with the nucleoside monophosphates dTMP5′, dTMP3′, dUMP5′, dGMP5′, uridine 2′-monophosphate (UMP2′); uridine 5′-monophosphate (UMP5′); and d4TMP. By combining the new structural information of substrate binding with activity measurements, we have been able to provide a structural explanation of why mdN prefers 2′-deoxyribonucleoside over ribonucleoside 5′-monophosphates and why it shows low activity for dGMP5′. The new information about substrate binding could potentially be used in the design of novel anti-HIV nucleoside analogs with reduced mitochondrial toxicity.

Results and Discussion

The D41N variant of mdN was prepared with the purpose of trapping various substrates in the active site of mdN. In the reaction mechanism of mdN (Rinaldo-Matthis et al., 2002), Asp-41 makes a nucleophilic attack on the phosphate moiety of the nucleoside monophosphate. In the D41N variant, residue Asp-41 is substituted by the poor nucleophile asparagine, which instead forms hydrogen bonds to the substrate, efficiently trapping it in the active site.

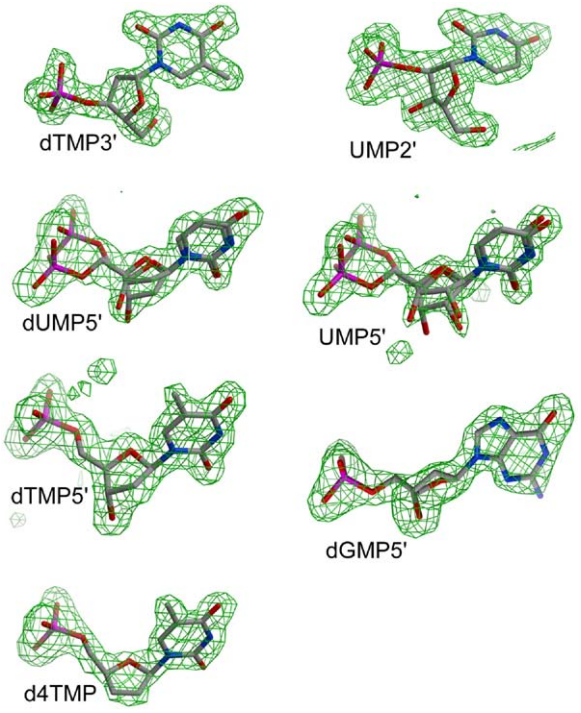

Figure 1. Electron Density and Bound Substrates

dUMP5′ and UMP5′ are modeled with the two alternate conformations superimposed. The OMIT maps are generated in Refmac5 (Murshudov et al., 1997).

Similar to the previously published mdN structures (Rinaldo-Matthis et al., 2002), the present structures contain 194 out of 197 residues (amino acids 34–227). Amino acids 1–31 constitute the mitochondrial localization signal and were not part of the expressed construct. It is a homodimer, and each monomer is composed of a large and a small domain. The active site of mdN is found in a cleft between the two domains and is solvent accessible. All present and previously solved structures contain a Mg^{2+} ion, to which either the inorganic phosphate, the phosphate moiety of the nucleotide, BeF_3^-, or AlF_4^- is coordinated (Rinaldo-Matthis et al., 2002; Rinaldo-Matthis, 2004). Many residues conserved between the known 5′-nucleotidases are situated around the phosphate binding site. These are Asp-41 (Asn-41), Asp-43, Lys-165, Asp-175, Asp-176, and Thr-130.

The electron density of the substrate is readily interpreted already in the initial Fo-Fc map, for all seven structures (Figure 1). In the structures with dUMP5′ and UMP5′, the density of the ribose and especially of the phosphate moiety is divided approximately equally over two locations, indicating the presence of two alternative conformations (Figure 1). Here, we describe these as two different phosphate binding modes, Mode

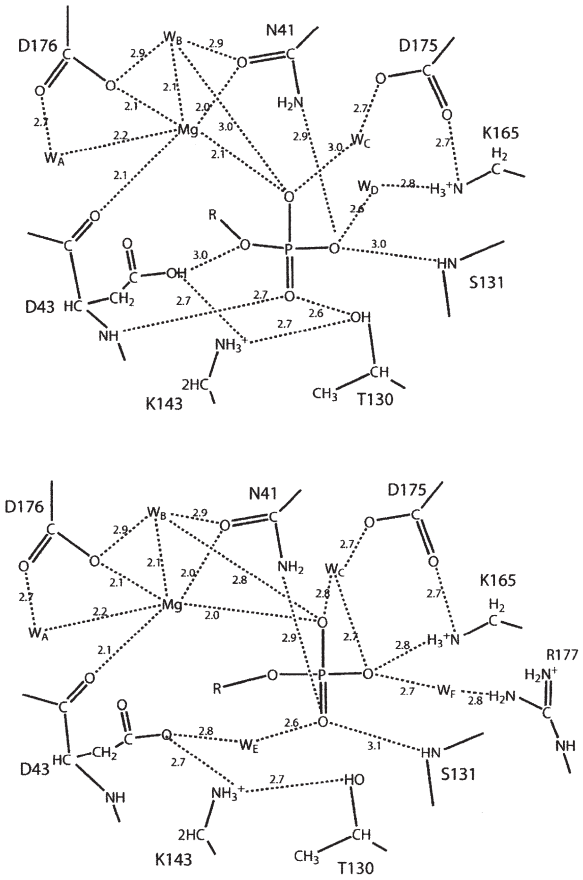

Figure 2. Schematic Diagrams of the Active Site of D41N

Top: Mode A, shown by the phosphate binding of dTMP3′. Bottom: Mode B, shown by the phosphate binding of dTMP5′. Waters are marked as "W."

A and Mode B (Figure 2). dTMP3′ and UMP2′ bind only with Mode A, dTMP5′ and d4TMP bind only with Mode B, and dGMP5′ is somewhat displaced from the phosphate binding site (see below).

The location of the phosphate in Mode A (Figure 2, top) is very similar to that of inorganic phosphate in a previously determined structure of wild-type mdN (Rinaldo-Matthis et al., 2002). The oxygen connecting the phosphate with the nucleoside (O5′) is within hydrogen bonding distance to Asp-43, a catalytically important residue that donates a proton to the leaving nucleoside product (Rinaldo-Matthis et al., 2002). The phosphate also makes hydrogen bonds to the amine group of Asn-41, the hydroxyl group of Thr-130, the main chain amide of Ser-131, and to several water molecules (W_B, W_C, and W_D). The phosphate is also coordinated to the Mg^{2+} ion. These interactions are similar to those between the wild-type mdN and inorganic phosphate/BeF_3^- described previously (Rinaldo-Matthis et al., 2002). However, Lys-165, which previously has been seen to coordinate to phosphate and BeF_3^-, is not making an interaction to the phosphate moiety in Mode A. A likely explanation for this could be that, since the negative charge of Asp-41 is removed in D41N, a close coordination of Lys-165 to the phosphate moiety would create an unfavorable charge distribution. It is likely that the D41N mutation has created a situation in which the conserved Lys-165 is not stabilizing the productive phosphate binding mode for catalysis, as has been suggested for wild-type mdN (Rinaldo-Matthis et al., 2002).

Mode B (Figure 2, bottom) shows a phosphate that "has rotated" around the C4′-C5′ bond of the ribose. We believe that Mode B is an artifact of the mutation, due to the changed charge distribution, and is not a biologically relevant situation. In Mode B, the O5′ is not within hydrogen bonding distance to Asp-43 or to any other possible proton donor, which indicates that this binding mode is nonproductive. Here, the phosphate makes a hydrogen bond to Lys-165. The phosphate moiety is not within hydrogen bonding distance to Thr-130, but it is coordinated to the Mg^{2+} ion and makes hydrogen bonds to the amine group of Asn-41 and to the main chain of Ser-131, as well as to several water molecules (W_B, W_C, W_E, and W_F). A water molecule (W_E) is situated between Asp-43 and the phosphate moiety within hydrogen bonding distance to Asp-43, but not to O5′. W_F connects the phosphate to Arg-177 (Figure 2, bottom).

In D41N, it is possible that the protonation state of Asp-43 determines whether the phosphate moiety will make a hydrogen bond to Asp-43 (Mode A) or to Lys-165 (Mode B). It is likely that the carboxyl group of Asp-43 is protonated in Mode A, where it makes a hydrogen bond to O5′, and is deprotonated in Mode B, where it repels the O5′ (Figure 2). It is evident from the present structures that several of the substrates can display both binding modes. The difference in phosphate binding could depend on the fact that the pKa values of the phosphate and Asp-43 are close to the pH of the crystal soaking solutions.

Since Mode A is almost identical to the binding of inorganic phosphate in wild-type mdN, and the sugar/base binding of dTMP3′ is almost identical to the binding of thymidine in wild-type mdN (Figure 3A) (Rinaldo-Matthis et al., 2002), the structures with Mode A most likely picture substrate binding very closely to how it actually occurs in vivo. The structure with dTMP3′ also verifies the conclusions previously drawn about substrate binding and the catalytic mechanism of the enzyme (Rinaldo-Matthis et al., 2002). Even though Mode B most likely is an artifact due to the changed charge distribution, the structures with Mode B are also relevant for understanding sugar and base binding, since only small changes in the conformation of the sugar moiety occur and almost no detectable conformational changes of the base are present (Figure 1).

Nucleoside 2′-, 3′-, and 5′-Monophosphate Binding

A comparison of the binding of UMP2′, dTMP3′, and dUMP5′ (Figures 3B and 3C) shows that the ribose and base of dUMP5′ are rotated relative to UMP2′ and dTMP3′. Here, dUMP5′ is representative also of UMP5′, dTMP5′, and d4TMP, since their base moieties bind very similarly and their ribose moieties bind relatively similarly (the differences in ribose binding between the nucleoside 5′-monophosphates will be discussed below).

The bases of dTMP3′ and UMP2′ bind almost identically and make only one direct hydrogen bond to the protein, which is between the O4 atom of the thymine/

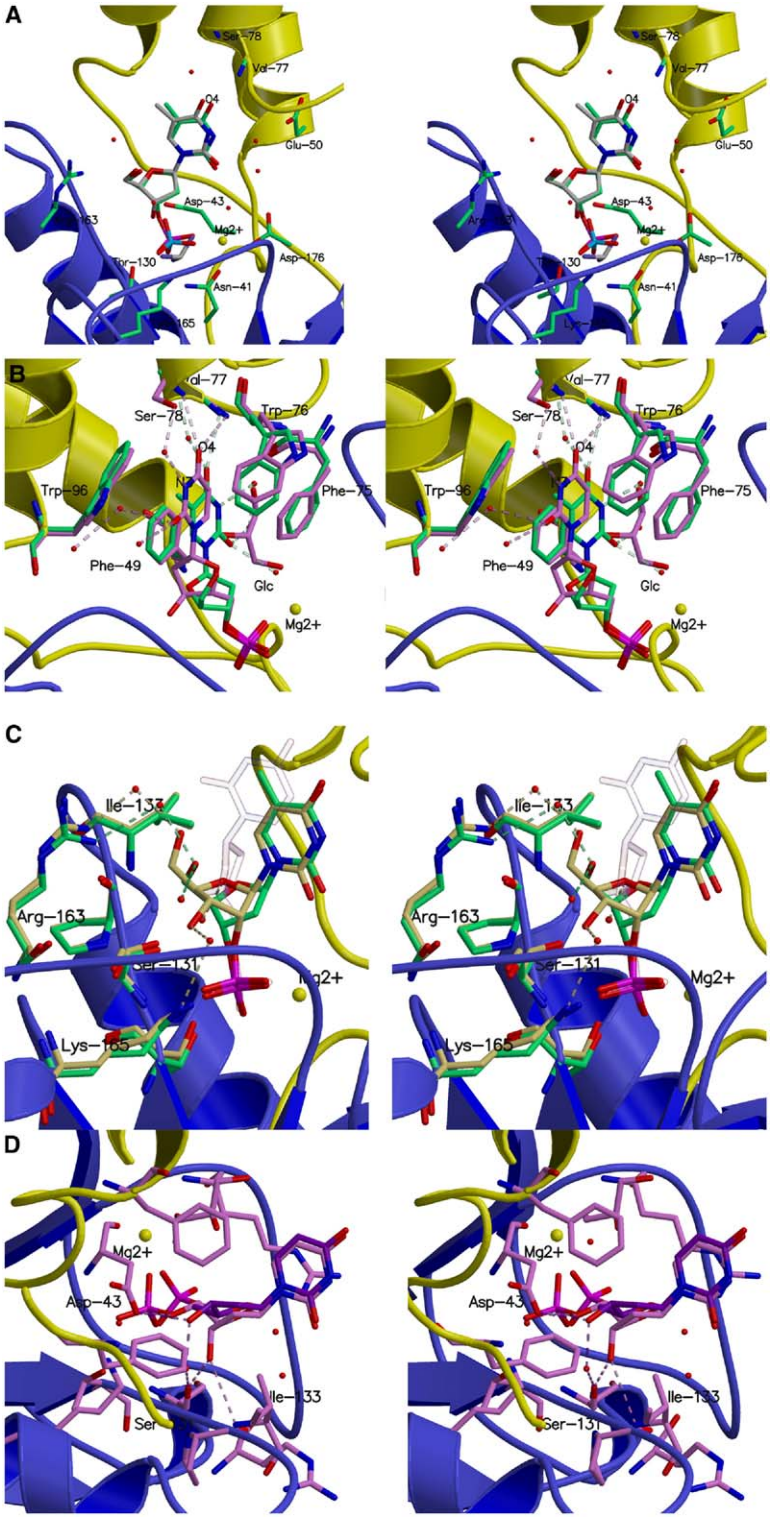

Figure 3. The Binding of UMP2′, dTMP3′, and dUMP5′

(A) Comparison of the binding of substrate, product, and inorganic phosphate. The substrate dTMP3′ is superimposed on the previously determined structures with the product thymidine together with BeF_3^-, and the native structure is superimposed with inorganic phosphate (Rinaldo-Matthis et al., 2002). dTMP3′ is shown in green, thymidine is shown in light gray, BeF_3^- is shown in light gray and indigo, and inorganic phosphate is shown in blue.

(B) Comparison of the base binding of dTMP3′ and dUMP5′ (Mode A), in stereo. The structures with dTMP3′ (green) and dUMP5′ (violet) are superimposed.

(C) A stereo view comparing the ribose binding of dTMP3′ and UMP2′. The structure with dTMP3′ (green) is superimposed on the structures with UMP2′ (yellow) and dUMP5′ (Mode A, transparent). No amino acid residues are shown from the structure with dUMP5′.

(D) Stereo view of the structure with dUMP5′, showing the two alternative conformations of dUMP5′. dUMP5′ (Mode A) is shown in violet, and dUMP5′ (Mode B) is shown in dark violet.

uracil ring and the amide group of Val-77. The thymine/uracil ring makes several interactions with water molecules that mediate contact with the Mg^{2+} ion and the protein (Figure 3B). The thymine ring of dTMP3′ (and the uracil ring of UMP2′) is stacked parallel to Phe-49 with a distance of 3.4 Å. It is also stacked parallel by Phe-75 (3.9 Å), and the 5-methyl group of thymine makes van der Waals interactions of 3.5 Å to both Trp-76 and Trp-96 (Figure 3B).

The O4 atom of the uracil ring of dUMP5′ makes hydrogen bonds to the amide group of Val-77, to the amide group of Ser-78, and to a water molecule that medi-

Table 1. Relative Activity of mdN and Kinetic Parameters

Substrate	Relative Activity[a]	K_m (mM)	V_{max} (Units/mg)	V_{max}/K_m
dUMP5′	100	0.16	145	909
UMP5′	30	0.14	46	323
UMP2′	18	0.05	30	600
dTMP5′	50	0.3	77	270
dTMP3′	77	0.17	144	833
dGMP5′	6	0.09	15	167
d4TMP5′[b]	9	0.3	14	47

[a] Values are taken from a previous publication (Rampazzo et al., 2000a) and were measured at pH 5.5 with a substrate concentration of 2 mM.
[b] Values are taken from a previous publication (Mazzon et al., 2003) and were measured at pH 7.5 with a substrate concentration of 2 mM.

ates interaction with the side chain of Ser-78 (Figure 3B). The uracil ring of dUMP5′ is stacked by Phe-49, Phe-75, Trp-76, and Trp-96, but to a lesser extent than the pyrimidine bases in dTMP3′ and UMP2′. The uracil ring is closer to Trp-76 and Trp-96 than to Phe-49, which is more than 4 Å away and is not stacked parallel to it. The N3 of the uracil ring of dUMP5′ is relatively close to non-polar parts of the two tryptophans. Phe-75 and Trp-76 have moved slightly relative to their positions in the structure with dTMP3′ (Figure 3B). The residues Phe-49, Phe-75, Trp-76, and Trp-96 form a pocket, which fits dTMP3′ very well, but fits the dUMP5′ (and all nucleoside 5′-monophosphates included in this study) less well.

One glycerol molecule that probably originates from the cryosolution used for freezing the protein crystals is found in the active site of the structure with dUMP5′, where it coordinates the Mg^{2+} ion (Glc in Figure 3B). None of the other structures included in this paper have glycerol bound at this position, and since the binding mode of dUMP5′ is so similar to the binding modes of UMP5′, dTMP5′, and d4TMP, it is most probable that the glycerol molecule is not affecting the binding mode of the substrates but rather fills positions normally occupied by water molecules.

The sugar moieties of dTMP3′ and UMP2′ bind to water molecules that mediate interaction with the protein (Figure 3C). The nucleoside 5′-monophosphates bind with two different sugar ring conformations, in which the 3′-hydroxyl group interacts with the enzyme in two different ways (Figure 3D): (1) In dUMP5′ (Mode A), UMP5′ (Mode A), and dTMP5′, the 3′-hydroxyl group makes hydrogen bonds to the main chain carbonyl group of Ser-131 and the main chain amide group of Ile-133. (2) In dGMP5′, dUMP5′ (Mode B), and UMP5′ (Mode B), it makes hydrogen bonds to the side chain carboxyl group of Asp-43 and to a water molecule. In both binding modes, the hydroxyl group makes direct interactions with the protein, leaving limited space for a putative bulky substituent, e.g., the azido group of the nucleoside analog AZT.

Four factors support the idea that not only nucleoside 5′-monophosphates, but also nucleoside 3′-monophosphates, are biologically relevant substrates. These are: (1) mdN has high activity for dTMP3′ (Table 1); (2) the stacking interactions of both dTMP3′ and

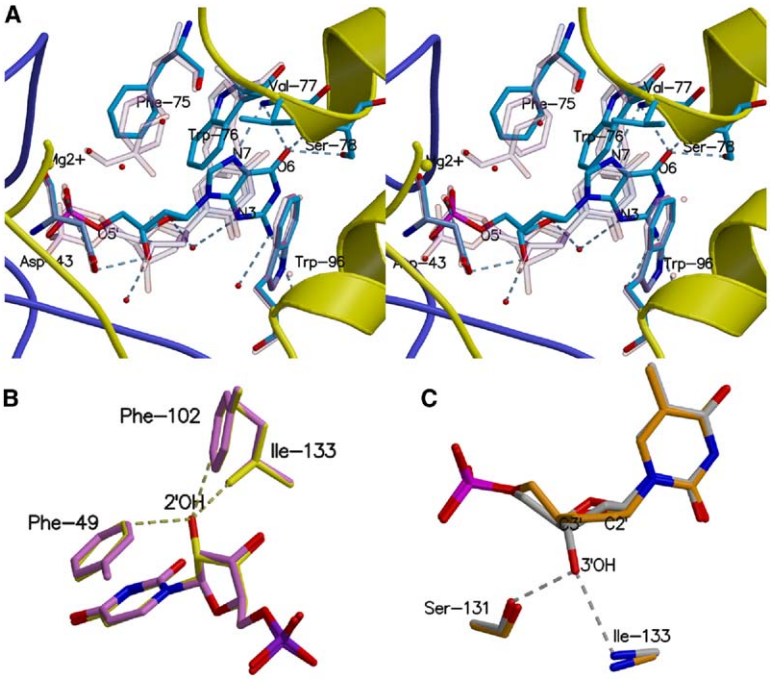

Figure 4. Comparisons of the Binding of Different Nucleoside 5′-Monophosphates

(A) Superposition of the structure with dGMP5′ (blue) and the structure with the two alternative conformations of dUMP5′ (transparent), in stereo.

(B) Superposition of the structures with dUMP5′ (purple) and UMP5′ (yellow).

(C) Superposition of the structures with dTMP5′ (light gray) and d4TMP5′ (orange).

Table 2. Crystallographic Data Collection and Refinement Statistics

Data Collection Parameters	Substrate						
	dTMP3′	dTMP5′	dUMP5′	UMP5′	UMP2′	dGMP5′	d4TMP5′
Space group	$P4_32_12$	$P4_32_12$	$P4_32_12$	$P4_32_12$	$P4_32_12$	$P4_32_12$	$P4_32_12$
Unit Cell Dimensions (Å)							
a = b	73.18	73.65	73.7	73.57	73.45	73.38	73.77
c	105.92	106.38	106.42	105.75	106.09	105.437	106.06
Data Collection Statistics							
Resolution (Å)	20–1.75	40–1.8	20–2.0	40–1.7	37–1.8	40–2.00	20–2.05
$I/\sigma(I)$[a]	15.9 (5.2)	17.7 (3.9)	23.6 (7.8)	24.5 (3.7)	27.3 (4.7)	25.5 (4.5)	21.5 (4.3)
Number of unique reflections	29,986	27,554	20,833	32,144	27,294	20,174	18,971
Redundancy of reflections	7.5	4.9	15.1	5.0	8.2	6.6	6.1
R_{sym}[a,b]	7.2 (32)	5.6 (35)	8.0 (36)	4.7 (33.4)	6.1 (37)	7.2 (45)	7.3 (37)
Completeness (%)[a]	92.7 (95.0)	99.4 (99.4)	99.8 (100)	98.5 (98.3)	98.4 (98.8)	99.6 (99.9)	99.7 (100)
Final Refinement Parameters							
R_{work} value[c]	17	17	16	19	17	19	17
Number of reflections, working set	26,334	26,283	19,762	30,463	25,876	19,103	17,970
R_{free} value[c]	18	21	20.6	21	20	21.5	21
Number of reflections, test set	1,420	1,383	1,069	1,624	1,369	1,027	976
Mean B factors (Å^2)	22.3	19.3	26.5	24.3	20.8	22.9	25.2
Residues in most favorable regions (%)[d]	92.9	92.9	92.4	91.8	92.9	91.8	92.4
Residues in additionally allowed regions (%)[d]	7.1	7.1	7.6	8.2	7.1	8.2	7.6
Rmsd bond length (Å)	0.018	0.019	0.019	0.015	0.018	0.019	0.02
Rmsd bond angles (°)	1.682	1.790	1.690	1.631	1.755	1.684	1.672
PDB code	1Z4K	1Z4L	1Z4I	1Z4M	1Z4J	1Z4P	1Z4Q

[a] Numbers in parentheses are for the highest resolution shell.
[b] $R_{sym} = (\Sigma_{hkl}\Sigma_i|I_i(hkl) - \langle I(hkl)\rangle|)/\Sigma_{hkl}\Sigma_i I_i(hkl)$ for n independent reflections and observations of a given reflection; $\langle I(hkl)\rangle$ is the average intensity of the i^{th} observation.
[c] $R_{cryst} = \Sigma_{hkl}|F_0(hkl) - F_c(hkl)|/\Sigma_h|F_0(hkl)|$.
[d] Ramachandran plots are made by using PROCHECK Validation (Laskowski et al., 1993).

UMP2′ are more favorable than those of the nucleoside 5′-monophosphates; (3) the two stacking phenylalanines (Phe-49 and Phe-75) are conserved between mdN and cdN, which indicates the biological importance of this stacking; and (4) in the previously solved structure of mdN in complex with the nucleoside product, the 3′-hydroxyl group of the nucleoside product is pointing toward the phosphate binding site, which indicates that the enzyme has higher affinity for nucleoside 3′-monophosphates than for nucleoside 5′-monophosphates.

Nucleoside 5′-Monophosphate Specificity

Purine/Pyrimidine Specificity

The activity of mdN is much lower with purine nucleotides, e.g., dGMP5′, than with the pyrimidine substrates dTMP5′ and dUMP5′ (Table 1). The difference is especially marked at saturating substrate concentrations. The structure of mdN with bound dGMP5′ reveals that dGMP5′ is displaced 1 Å relative to the other nucleoside 5′-monophosphates, which causes a longer distance (4.4 Å) between O5′ and the catalytically important Asp-43 (Figure 4A) than in the other substrate-D41N complexes that display Mode A. This longer distance to Asp-43 probably makes the transfer of a proton from Asp-43 to the leaving nucleoside in the reaction mechanism less efficient, and thus causes the low activity of mdN with dGMP5′. The phosphate moiety of dGMP5′ overlaps with that of Mode B, but a rotation around the C5′-O5′ bond of the nucleotide would not place the phosphate in a location similar to Mode A, since the location of the sugar ring and the rest of the nucleotide prohibits the phosphate moiety from reaching Mode A.

The O6 of the guanine ring of dGMP5′ makes hydrogen bonds to the amide of Val-77 and to the amide and hydroxyl groups of Ser-78. The N7 of the guanine ring makes a hydrogen bond to the amide group of Val-77, and the O4′ of the ribose moiety and the amide group of the guanine ring make hydrogen bonds to water molecules (Figure 4A). It is probable that the interactions with Val-77 and Ser-78 cause the displacement of dGMP5′, and thus the preference for pyrimidines over purines.

Deoxyribo/Ribo Specificity

The deoxyribonucleotidase mdN prefers the 2′-deoxyribo form of nucleoside 5′-monophosphates and shows lower catalytic efficiency with the corresponding ribo form, e.g., UMP5′ (Table 1). The substrates UMP5′ and dUMP5′ bind remarkably similarly in the D41N variant (Figure 4B). However, the 2′-hydroxyl group of UMP5′

is positioned in a hydrophobic pocket, where it is 3.5 Å from Phe-49, 3.5 Å from Phe-102, and 2.6 Å from Ile-133, all energetically unfavorable interactions. For dUMP5′, on the other hand, these hydrophobic residues constitute a favorable surface for interactions with the 2′-carbon, which suggests that dUMP5′ is bound with higher affinity than UMP5′. However, judging from the kinetic parameters for these two substrates in Table 1, this difference in the interactions with the enzyme affects the Vmax, but not the K_ms, which are the same for dUMP5′ and UMP5′.

Importance of the 3′-Hydroxyl Group of dNMP5's

The 5′-monophosphate of the anti-HIV thymidine analog d4T (d4TMP) is a poor substrate for mdN (Table 1). d4TMP lacks the 3′-hydroxyl group that is present in dTMP5′ and has a double bond between the C2′ and C3′ atoms. Even though the double bond makes the conformation limited to O4-endo envelope puckering, the sugar ring still occupies similar space as the sugar ring of dTMP5′. The 3′-carbons of d4TMP and dTMP5′ are in a similar position and the bases bind almost identically. The only detectable difference in the interactions with the enzyme is that dTMP5′ has two additional hydrogen bonds: the hydrogen bonds between the 3′-hydroxyl group and the carbonyl group of Ser-131 and the amide group of Ile-133. These hydrogen bonds are most likely more favorable than the exposure of the 3′-carbon of d4TMP to this polar environment, which is in agreement with the difference in relative activity between the two substrates (Table 1). The lack of a polar group at the 3′ position of the sugar would probably in general destabilize the binding in mdN, causing a lower V_{max}.

Nucleoside Analog Specificity

The binding of the nucleoside 5′-monophosphates reveals that the parts of the base that are not involved in direct interactions with the protein are surrounded by water molecules, which could potentially be substituted by other solvent molecules (e.g., glycerol; Figure 3B) or by a functional group of a nucleoside analog. The structures with UMP5′ and d4TMP indicate that a nucleoside analog should have a small polar or charged group at the 3′ position of the ribose and have no polar or charged functional group at the 2′ position of the ribose, in order to maintain activity.

Possibly, a nucleoside analog that is substituted on the base (with the exception of the O4 position) is more likely to be a good substrate for mdN than one substituted on the ribose.

Experimental Procedures

Site-Directed Mutagenesis

Site-directed mutagenesis of mdN was performed as described by Sambrook and Russel (2001). We used two complementary oligonucleotides to introduce the mutation: 5′-gccgtccatgttcacca gcaccc-3′ and 5′-gggtgctggtgaacatggacggc-3′ (small letters indicate wild-type bases; bold letters indicate mutated bases). As external primers we used 5′-catacatatgggaggccgcgccctacg-3′ and 5′-ctgaggatccagccccacagagga-3′, which introduce a 5′ NdeI and a 3′ BamHI site, respectively (underlined). After PCR amplification, the mutated cDNA lacking the codons for the 31 N-terminal amino acids with the mitochondrial targeting signal was cloned into pET20 vector (Novagen, Madison, WI, USA). The recombinant plasmid, called pET20-D41NmdN, was sequenced to confirm the presence of the mutation.

Protein Expression and Purification

Plasmid pET20-D41NmdN was transformed into *Escherichia coli* BL21(DE3) plysS . The bacterial culture (9 L) was grown at 37°C in LB medium to an OD_{600} of 0.5–0.6 and was induced with 0.4 mM isopropyl-β-D-thiogalactoside for 3 hr. Extracts were prepared as described previously (Rampazzo et al., 2000b), and the D41N variant of mdN was purified by following the same procedure as that used previously for wild-type mdN (Rampazzo et al., 2000a). Briefly, the enzyme was purified by ammonium sulfate fractionation, chromatographed on a DE52 column (Whatman) with a 0–150 mM NaCl gradient in buffer A (20 mM Tris-HCl [pH 7.5], 1 mM EDTA [pH 7.6], 2 mM DTT, and 20% [v/v] glycerol). The peak was rechromatographed on a Phenyl Sepharose CL-4B column (Amersham Pharmacia) with a 1.5–0 M gradient of ammonium sulfate in buffer A. The peak was loaded again in a desalting biogel column (BioRad) in order to remove ammonium sulfate.

Enzyme Assays

Dephosphorylation of nucleotides was measured with a sensitive colorimetric assay from the formation of inorganic phosphate (Geladopoulos et al., 1991). Incubations were at 37°C for 30 min with substrate, 10 mM Mg^{2+}, 30 mM KCl, and 250 mM acetate buffer (pH 5.5) in a final volume of 50 μl. The reaction was stopped by the addition of 1/8 volume H_2SO_4 (1.1 M), and, after centrifugation, inorganic phosphate was determined. One unit of enzyme activity corresponds to the dephosphorylation of 1 μmol substrate per minute. Specific activity is units per mg protein. K_m and V_{max} values were obtained from the extrapolated maximal specific activity of the Lineweaver-Burk plots. All experiments were done in triplicate at different concentrations of the substrate and were repeated at least three times. In all kinetic experiments, care was taken not to consume more than 25% of the substrate during the reaction.

Crystallization, Soaking Experiments, and Cryoprotection

The D41N variant of mdN was crystallized under the same conditions as those described for mdN (Rinaldo-Matthis et al., 2002). The protein solution used for crystallization contained 20 mM Tris buffer (pH 7.5), 20% (v/v) glycerol, 2 mM DTT, 1 mM EDTA, 75 mM NaCl, and 10.1 mg ml^{-1} protein. Crystals were obtained by using the hanging drop vapor diffusion method with 1 μl protein solution and 1 μl reservoir solution at 20°C. The reservoir solution contained 15%–20% (w/v) PEG 8000 and 50 mM KH_2PO_4 (pH 4.5). Crystals appeared after 1 day and reached a maximum size of 0.2 × 0.2 × 0.3 mm. The D41N crystals were soaked in 10 μl drops containing 10 mM nucleoside monophosphate, 90 mM $MgCl_2$, 50 mM sodium acetate (pH 4.5), and 20% (w/v) PEG 8000 for 1–2 hr. The pH of the nucleoside monophosphate solutions was adjusted to pH 5 prior to soaking. The crystals were then transferred to a 10 μl drop of cryosolution containing 20% (w/v) PEG 8000, 50 mM sodium acetate (pH 4.5), and 20% (v/v) glycerol for 20–60 s and subsequently flash frozen in liquid N_2. For the structure with dGMP5′, 20% PEG 400 (v/v) was used instead of glycerol in the cryosolution.

Data Collection, Structure Determination, and Refinement

The data sets of D41N in complex with dTMP3′ and dUMP5′ were collected at the European Synchrotron Radiation Facility (ESRF) at the beamline ID14.3, the data set of D41N in complex with dGMP5′ was collected at the Protein Structure Factory-Berliner Elektronenspeicherring-Gesellschaft für Synchrotron Strahlung m. b. H. (PSF-BESSY) at beamline BL1, and the data sets of D41N in complex with UMP5′, UMP2′, dTMP5′, and d4TMP were collected at The European Molecular Biology Laboratory (EMBL) Hamburg Outstation at the beamline X11. The data sets with dTMP3′ and dUMP5′ were processed with XDS and XSCALE (Kabsch, 1988); the other data sets were processed by using the program package DENZO/SCALEPACK (Otwinowski and Minor, 1997). The crystals belong to the space group $P4_32_12$, with one polypeptide per asymmetric unit.

Refmac5 (Murshudov et al., 1997) was used for structure determination and refinement, and the previously determined mdN structure (Rinaldo-Matthis et al., 2002) was used as a template for the initial Rigid Body refinement of the seven data sets. Quanta (Accelrys, San Diego, CA) was used for model building, and X-SOL-

VATE (Accelrys) was used for the addition of waters. Structural statistics are shown in Table 2.

Acknowledgments

We would like to thank the staff at beamline ID14.3 at ESRF, at beamline X11 at the EMBL Hamburg Outstation and at beamline BL1 at PSF-BESSY for technical assistance. This work was supported by grants from Telethon Italia (V.B.), Associazione Italiana per la Ricerca sul Cancro (AIRC) (V.B.), the Swedish Research Council (P.N.), the Swedish Cancer Society (P.N.), and from The European Commission Grant nr.QLGI-CT-2001-01004 (P.N. and V.B.).

Received: October 29, 2004
Revised: March 16, 2005
Accepted: April 23, 2005
Published: July 12, 2005

References

Bianchi, V., and Spychala, J. (2003). Mammalian 5′-nucleotidases. J. Biol. Chem. *278*, 46195–46198.

Bradshaw, H.D., Jr., and Deininger, P.L. (1984). Human thymidine kinase gene: molecular cloning and nucleotide sequence of a cDNA expressible in mammalian cells. Mol. Cell. Biol. *4*, 2316–2320.

Feng, J.Y., Johnson, A.A., Johnson, K.A., and Anderson, K.S. (2001). Insights into the molecular mechanism of mitochondrial toxicity by AIDS drugs. J. Biol. Chem. *276*, 23832–23837.

Gallinaro, L., Crovatto, K., Rampazzo, C., Pontarin, G., Ferraro, P., Milanesi, E., Reichard, P., and Bianchi, V. (2002). Human mitochondrial 5′-deoxyribonucleotidase. Overproduction in cultured cells and functional aspects. J. Biol. Chem. *277*, 35080–35087.

Gazziola, C., Ferraro, P., Moras, M., Reichard, P., and Bianchi, V. (2001). Cytosolic high Km 5′-nucleotidase and 5′(3′)-deoxyribonucleotidase in substrate cycles involved in nucleotide metabolism. J. Biol. Chem. *276*, 6185–6190.

Geladopoulos, T.P., Sotiroudis, T.G., and Evangelopoulos, A.E. (1991). A malachite green colorimetric assay for protein phosphatase activity. Anal. Biochem. *192*, 112–116.

Höglund, L.R., and Reichard, P. (1990). Cytoplasmic 5′(3′)-nucleotidase from human placenta. J. Biol. Chem. *265*, 6589–6595.

Johansson, M., and Karlsson, A. (1997). Cloning of the cDNA and chromosome localization of the gene for human thymidine kinase 2. J. Biol. Chem. *272*, 8454–8458.

Johnson, A.A., Ray, A.S., Hanes, J., Suo, Z.C., Colacino, J.M., Anderson, K.S., and Johnson, K.A. (2001). Toxicity of antiviral nucleoside analogs and the human mitochondrial DNA polymerase. J. Biol. Chem. *276*, 40847–40857.

Jordan, A., and Reichard, P. (1998). Ribonucleotide reductases. Annu. Rev. Biochem. *67*, 71–98.

Kabsch, W. (1988). Automatic-indexing of rotation diffraction patterns. J. Appl. Crystallogr. *21*, 67–71.

Lai, Y.R., Tse, C.M., and Unadkat, J.D. (2004). Mitochondrial expression of the human equilibrative nucleoside transporter 1 (hENT1) results in enhanced mitochondrial toxicity of antiviral drugs. J. Biol. Chem. *279*, 4490–4497.

Laskowski, R.A., Macarthur, M.W., Moss, D.S., and Thornton, J.M. (1993). Procheck—a program to check the stereochemical quality of protein structures. J. Appl. Crystallogr. *26*, 283–291.

Lewis, W., and Dalakas, M.C. (1995). Mitochondrial toxicity of antiviral drugs. Nat. Med. *1*, 417–422.

Lim, S.E., and Copeland, W.C. (2001). Differential incorporation and removal of antiviral deoxynucleotides by human DNA polymerase gamma. J. Biol. Chem. *276*, 23616–23623.

Marinaki, A.M., Escuredo, E., Dudley, J.A., Simmonds, H.A., Amici, A., Naponelli, V., Magni, G., Seip, M., Ben-Bassat, I., Harley, E.H., et al. (2001). Genetic basis of hemolytic anemia caused by pyrimidine 5′ nucleotidase deficiency. Blood *97*, 3327–3332.

Mazzon, C., Rampazzo, C., Scaini, M.C., Gallinaro, L., Karlsson, A., Meier, C., Balzarini, J., Reichard, P., and Bianchi, V. (2003). Cytosolic and mitochondrial deoxyribonucleotidases: activity with substrate analogs, inhibitors and implications for therapy. Biochem. Pharmacol. *66*, 471–479.

Murshudov, G.N., Vagin, A.A., and Dodson, E.J. (1997). Refinement of macromolecular structures by the maximum-likelihood method. Acta Crystallogr. D Biol. Crystallogr. *53*, 240–255.

Otwinowski, Z., and Minor, W. (1997). Processing of X-ray diffraction data collected in oscillation mode. Methods Enzymol. *276*, 307–326.

Rampazzo, C., Gallinaro, L., Milanesi, E., Frigimelica, E., Reichard, P., and Bianchi, V. (2000a). A deoxyribonucleotidase in mitochondria: involvement in regulation of dNTP pools and possible link to genetic disease. Proc. Natl. Acad. Sci. USA *97*, 8239–8244.

Rampazzo, C., Johansson, M., Gallinaro, L., Ferraro, P., Hellman, U., Karlsson, A., Reichard, P., and Bianchi, V. (2000b). Mammalian 5′(3′)-deoxyribonucleotidase, cDNA cloning, and overexpression of the enzyme in *Escherichia coli* and mammalian cells. J. Biol. Chem. *275*, 5409–5415.

Rampazzo, C., Ferraro, P., Pontarin, G., Fabris, S., Reichard, P., and Bianchi, V. (2004). Mitochondrial deoxyribonucleotides, pool sizes, synthesis and regulation. J. Biol. Chem. *279*, 17019–17026.

Rinaldo-Matthis, A. (2004). Crystal structures of human deoxyribonucleotidases. PhD thesis, Stockholm University, Stockholm, Sweden.

Rinaldo-Matthis, A., Rampazzo, C., Reichard, P., Bianchi, V., and Nordlund, P. (2002). Crystal structure of a human mitochondrial deoxyribonucleotidase. Nat. Struct. Biol. *9*, 779–787.

Sambrook, J., and Russel, D.W. (2001). Molecular Cloning: A Laboratory Manual, Third Edition (New York: Cold Spring Harbor Press).

Tozser, J. (2001). HIV inhibitors: problems and reality. Ann. N. Y. Acad. Sci. *946*, 145–159.

Van Rompay, A.R., Johansson, M., and Karlsson, A. (2003). Substrate specificity and phosphorylation of antiviral and anticancer nucleoside analogues by human deoxyribonucleoside kinases and ribonucleoside kinases. Pharmacol. Ther. *100*, 119–139.

Wang, L., Munch-Petersen, B., Sjoberg, A., Hellman, U., Bergman, T., Jornvall, H., and Eriksson, S. (1999). Human thymidine kinase 2: molecular cloning and characterisation of the enzyme activity with antiviral and cytostatic nucleoside substrates. FEBS Lett. *443*, 170–174.